PNAS
www.pnas.org

Supplementary Information for

Role of UCHL1 in axonal injury and functional recovery after cerebral ischemia

Hao Liu[1,2*], Nadya Povysheva[3*], Marie E. Rose [1,2], Zhiping Mi[1,2], Joseph S. Banton[2], Wenjin Li[2], Fenghua Chen[2], Daniel P. Reay[1,2], Germán Barrionuevo[3], Feng Zhang [1,2] and Steven H. Graham[1,2]

Paste corresponding author name: Steven H. Graham and Feng Zhang
Email: Steven H. Graham: Steven.Graham@va.gov
Feng Zhang: ZhanFx2@upmc.edu

This PDF file includes:

Supplementary text
Figs. S1 to S5
References for SI reference citations

www.pnas.org/cgi/doi/10.1073/pnas.1821282116

Materials and methods

Animal studies were performed in accordance with the recommendations in the Guide for the Care and Use of Laboratory Animals of the National Institutes of Health. The protocol was approved by the University of Pittsburgh Institutional Animal Care and Use Committee (Protocol Number: IS00001941). All surgery was performed under isoflurane anesthesia, and all efforts were made to minimize suffering. Animals were housed in a temperature and humidity-controlled environment with 12 h light cycles and free access to food and water. Surgeries, assessment of behavioral outcome and analysis of tissue loss were performed by blinded researchers.

Reagents and Antibodies:

Antibodies used in this study were obtained from the following companies: mouse monoclonal anti-poly-ubiquitinated conjugates (clone FK1) was from Enzo Life Sciences (Plymouth Meeting, PA); anti-ubiquitin (linkage-specific K63), anti-19S and anti-20S proteasome subunits, anti-ubiquitin and anti-myelin basic protein (MBP) were from Abcam (Cambridge, MA); anti-ubiquitin (K48-specific), and anti-neurofilament H non-phosphorylated mAb (SMI-32) were purchased from Millipore (Temecula, CA); anti-LC3B and anti-Beclin-1 rabbit antibodies were from Cell Signaling Technology (Boston, MA); monoclonal anti-GAPDH was from Covance (Berkeley, CA); DyLight549- or Alexafluor 488-conjugated secondary antibodies were from Jackson Immunoresearch Lab (West Grove, PA). Anti-β-actin antibody and all other chemicals were from Sigma-Aldrich.

***In vitro* hypoxia, oxygen and glucose deprivation (OGD) and cell death measurements:**

Hypoxic conditions were induced by exposing cultures to 92% argon, 5% CO_2, and 3% H_2 for 2-3 hours using an anaerobic chamber (Coy Laboratories, Grass Lake, MI) as described previously resulting in ~40% cell death after 24 h reperfusion(1). Cells treated with staurosporin (20 μM, a 100% cell death internal standard) and 1 μM dizocilpine (MK801, a 100% cell survival internal standard) were included in each cell death assay experiment. OGD was performed as previously described(2). Cells were incubated in buffered Hanks' solution lacking glucose prior to exposure to hypoxic conditions. Cell death was quantitatively assessed by measuring lactate dehydrogenase (LDH) release into the culture medium 24 h after hypoxia or indirectly through the 3-(4,5-dimethylthiazol-2-yl)-2,5-diphenyltetrazolium bromide (MTT) cell viability assay (n = 6-12 wells per group). Cell death was also measured by staining cells with 0.1 μg/ml propidium iodide (PI) and 0.1 μg/ml Hoechst, followed by fixation with 2% formaldehyde in phosphate buffered saline (PBS) 24 h after hypoxia. PI and Hoechst stained cells were counted from 10-12 fields of at least three cultures using a fluorescence microscope with appropriate filters. Data are expressed as percentage PI-stained cells.

***In vitro* axonal injury analysis:**

In vitro axonal injury analysis was performed as described previously with minor modifications(3). Primary neurons from wild type or UCHL1 C152A knock-in mice were seeded onto L-poly D-lysine-coated glass coverslips. 24 h after hypoxia, cells were fixed with 4% paraformaldehyde (PFA) in PBS and were immunostained with anti-

Neurofilament-L antibody (1:100, Cell Signaling Technology #2837) and Alexafluor 488-conjugated secondary antibody sequentially, then photographed at 60X using a confocal microscope (Olympus, Tokyo, Japan). Analysis was performed on cells randomly selected from 2 coverslips for each treatment condition (hypoxia or normoxia) per genotype (n = 8 fields per group). Quantification of axon degeneration was performed by a blinded investigator as previously described(4, 5). Axon/neurite outgrowth was evaluated based on morphological characteristics: 1) intact: length of axon/neurite outgrowth > 2X the length of the soma; 2) fragments: isolated neurite segments. The numbers of intact neurites and neurites fragments were normalized to the number of neurons examined.

Middle cerebral artery occlusion (MCAO):

Male mice, aged 10 – 12 weeks, were used for MCAO studies. Anesthetic induction was achieved using inhaled 4% isoflurane in 50% nitrous oxide, balance oxygen, then lowered to 1.5% throughout surgery. Core body temperature was maintained at 37 +/- 0.5 ^{o}C using a water-filled heating pad. MCAO was induced in WT and KI male mice, by making a midline incision at the trachea, retracting soft tissues and advancing a nylon suture into the MCA for a duration of 60 min as previously described with some modifications(6). Sham surgeries were performed identically, without insertion of the occluding suture, for the same anesthetic duration. Animals were monitored continuously during anesthetic induction and surgery, and for 30 min. following reperfusion, with daily monitoring thereafter. Bupivacaine (0.25%) was applied to the wound after MCAO suture removal and wound closure. Mouse euthanasia for immunoblotting was performed using isoflurane anesthesia followed by decapitation.

Core infarct and penumbral brain tissues were rapidly dissected and frozen for analysis. For immunohistochemical studies, mice were euthanized by insufflating a chamber with CO_2 followed by brain perfusion fixation via the left ventricle with heparinized saline followed by formalin. Mouse brain preparation for electrophysiology studies was as follows: mice were deeply anesthetized with chloral hydrate and decapitated. The brain was quickly removed and immersed in ice-cold pre-oxygenated artificial cerebrospinal fluid (ACSF). A tissue block containing the ischemic core was excised for slicing. Coronal slices (350-400 μm thick) were cut with a vibratome (Leica VT1000S, Leica, Germany). Slices were incubated at 37°C for 0.5-1 h and further stored at room temperature until they were transferred to a recording chamber perfused with ACSF at 31-32°C. Through all steps of the experiments, ACSF of the following composition was used (in mM): 126 NaCl, 2.5 KCl, 1.25 NaH_2PO_4, 1 $MgSO_4$, 2 $CaCl_2$, 24 $NaHCO_3$, 10-20 glucose; pH 7.25-7.3. ACSF was perfused with a 95% O_2/5% CO_2 gas mixture.

Behavioral assessment:

Mouse four limb symmetry and forelimb outstretch testing was performed using methods established by Garcia et al(7). Symmetry of movement of the mouse's four limbs was measured on Day 0 (baseline) and D1 – D5 post MCAO. The mouse was held in the air by the tail and scoring was as follows: 3, all four limbs extended symmetrically; 2, limbs on left side extended less or more slowly than those on the right; 1, limbs on left side showed minimal movement; and 0, forelimb on left side did not move at all. Three trials per day were run. N = 8-9 mice per group. Forelimb symmetry: The mouse was brought to the edge of the table and made to walk on its forelimbs while being held by the tail. Symmetry in the outstretching of both forelimbs was noted while

the mouse reached for the table surface and the hindlimbs were kept in the air with scores as follows: 3, both forelimbs were outstretched with the animal walking symmetrically on both forepaws; 2, the contralateral side outstretched less than the right, and forepaw walking was impaired; 1, the contralateral forelimb moved minimally; and 0, the contralateral forelimb did not move. Cylinder Test: Cylinder testing was performed using methods outlined by Schallert and Hua et al(8, 9). Sensorimotor outcome was assessed on days 20-23 post injury. Mice were placed in a clear plexiglass cylinder 10 cm in diameter and 25 cm high for 10 min. Forelimb placement during rearing and landing activities was video-recorded. Scoring was performed as follows: (a) independent use of the left or right forelimb for contacting the wall during a full rear, to initiate a weight-shifting movement or to regain center of gravity while moving laterally in a vertical posture; (b) independent use of the left or right forelimb to land after a rear: (c) simultaneous use of both the left and right forelimb for contacting the wall of the cylinder during a full rear and for lateral movements along the wall; (d) simultaneous use of both the left and right forelimb for landing following a rear. If limb use could not be determined, that movement was not scored. Behavioral data are shown as means ± SEM. N = 9-10 mice per group.

Brain tissue preparation and Western blotting:

Brain tissue dissection and Western blotting were performed as previously described(10). Ipsilateral and contralateral brain cortex penumbra were dissected from mice at 24h and 7d post-MCAO/ sham procedure and rapidly frozen on dry ice until homogenization with N-PER tissue protein extraction reagent (Pierce) supplemented with protease and phosphatase inhibitors. Protein concentrations were measured by

BCA assay. Cell lysates were resolved on a 4-20% linear gradient polyacrylamide gel (BioRad, Hercules, CA) before incubation with indicated first antibodies. Blots were washed and the appropriate secondary antibodies applied. Protein signal was visualized with ECL reagents (Pierce). Blots were also probed using anti-GAPDH or β-actin antibodies for verification of equal protein loading. N = 7-10 per group. Densitometric analysis was performed using ImageJ 1.50i software and results are normalized to the corresponding contralateral band.

Tissue loss measurement:

Mice were euthanized at 21 d after MCAO using CO_2 followed by brain perfusion fixation with 4% paraformaldehyde then embedded in paraffin. Sections were obtained every 0.5 mm. Slides were stained with hematoxylin and eosin (HE) and tissue loss was measured using ImageJ (U. S. National Institutes of Health, Bethesda, MD, USA). To minimize the effect of edema on the quantification of tissue volume, the method of Swanson et al. (11) was used: Tissue loss is calculated by subtracting surviving gray matter volume in lesioned hemispheres from gray matter volumes in unlesioned hemispheres and is expressed as percent unlesioned gray matter volume. N = 8 – 9 per group.

Fluorescent immunohistochemistry:

Myelin basic protein (MBP) and non-phosphorylated neurofilament H (SMI-32) immunofluorescent staining was performed as previously described (12, 13). Mice were sacrificed 7 d and 21 d after injury and coronal brain sections at bregma –1.9 mm were dual immunostained with anti-MBP Antibody (1:300) and anti- SMI-32 (1:500) then

incubated with AlexaFluor 488-conjugated goat anti-rabbit and Invitrogen CY3 goat anti-mouse secondary antibodies, respectively. Sections were photographed using an Olympus Fluoview confocal and Olympus BX51 microscopes with appropriate filters. MBP and SMI-32 fluorescence intensity was measured in corpus callosum in a 400 μm x 400 μm field at the center of the infarct, and in cortex in a 1.5 mm x 0.5 mm field, 1 mm from midline using ImageJ software. N = 8-10 animals per group. Brain sections incubated without application of primary antibody served as controls.

Electrophysiological recordings:

Whole-cell recordings were made from pyramidal neurons in layer 2-3 of the mouse neocortex 7 d and 21 d post ischemia, visualized by IR-DIC videomicroscopy using a Zeiss Axioskop microscope (Carl Zeiss, Inc., Thornwood, NY), with a 40x water immersion objective and a digital video camera (CoolSnap, Photometrics, Tucson, AZ). The neurons were located in close proximity to the ischemic core in MCAO-operated mice (1.0 mm from the edge of the infarct and 1.5 to -1.7 mm from bregma); comparably located neurons were selected in sham-operated animals. Pyramidal neurons were identified by their apical dendrites and triangular somata. Patch electrodes were filled with an internal solution containing: 120 mM K-gluconate, 2 mM MgCl2, 10 mM NaCl, 10 mM HEPES, 0.2 mM EGTA, 14 mM phosphocreatine, 4 mM ATP-Mg, 0.3 mM GTP-Na; pH 7.25. Alexa hydrazide 568 (0.075%; Molecular Probes, Eugene, OR) was added to the solution for later morphological identification of the recorded neurons. Electrodes had 5-10 MΩ open-tip resistance. Voltage and current recordings were performed with a Multi-Clamp 700A amplifier (Axon Instruments, Union City, CA). Voltage recordings were performed in bridge-balance mode. Signals were filtered at 2 kHz, and acquired at

a sampling rate of 10 kHz using a Digidata 1440 digitizer and Clampex l0.2 software (Molecular Devices Corporation, Sunnyvale, CA). Access resistance and capacitance were compensated on-line. Access resistance typically was 10-20 MΩ and remained relatively stable during experiments (≤ 30% increase) for the cells included in the analysis. Membrane potential was corrected for the liquid junction potential of -13 mV. Gabazine (10 μM; Ascent Scientific LTD, Bristol, UK) was used to inhibit $GABA_A$ receptors and tetrodotoxin (TTX; 0.5 μM; Sigma) was used to inhibit voltage-gated Na^+ channels.

Assessment of excitatory inputs:

Spontaneous excitatory post-synaptic currents (sEPSCs, n = 9-12 per group) were recorded at a holding potential of -70 mV. Miniature excitatory post-synaptic currents (mEPSCs, n = 6 – 12 per group) were recorded at a holding potential of -70 mV in the presence of TTX to inhibit action potential-mediated excitatory postsynaptic currents. Spontaneous and miniature events were analyzed using the MiniAnalysis Program (Synaptosoft, Decatur, GA). Peak events were first detected automatically using an amplitude threshold of 1.5 times the average route mean square (RMS) noise, which was ~3 pA for recordings at -70 mV holding potential. More than 500 events in each cell were included in the analysis.

Analysis of intrinsic membrane properties:

Membrane properties of neurons were analyzed using the Clampfit 10.2 software package (Molecular Devices Corporation, Sunnyvale, CA). To characterize the membrane properties of neurons, hyper- and depolarizing current steps were applied for

500 ms in 5-10 pA increments at 0.5 Hz. Series of depolarizing current steps of gradually increasing amplitude were used to evoke action potentials. Action potential properties were quantified using the first evoked action potential, defined as a regenerative depolarization with a maximum slope of at least 10 mV/ms. Action potential threshold was defined as the level of voltage deflection exceeding 10 mV/1 ms. Peak amplitudes of the action potential and of the afterhyperpolarization were measured relative to the action potential threshold. Duration of the action potential was measured at its half amplitude. Firing frequency was calculated in Hz as a ratio between number of action potentials and current step duration. N = 10 – 14 per group.

Estimation of axonal conduction velocity:

To estimate axonal conduction velocity, compound action potentials (CAPs) were evoked in the corpus callosum (14, 15) 7 d and 21 d post ischemia. A glass electrode filled with ASCF was used as the recording electrode, and a concentric bipolar electrode was used as a stimulating electrode. The stimulating electrode was placed ipsilateral to the MCAO affected area, and the extracellular recording electrode was placed contralateral to the MCAO site in the corpus callosum (Fig.3 C). An A360 Stimulus Isolator (World Precision Instruments, Sarasota, FL) was used to generate current stimuli that were triggered digitally with the PClamp software.

We used the approach by Reeves at al. (15) that enabled separate quantification of CAPs generated by two populations of callosal axons: relatively fast conducting fibers, corresponding to large, myelinated axons, and slower conducting unmyelinated, small-caliber fibers. Axonal conduction velocity was estimated as the ratio of the distance

between recording and stimulating electrode and the time between the onset of stimulation and the first negative peak for the myelinated fibers response and the second peak for the unmyelinated fibers response. N = 12-17 per group.

Labeling of pyramidal neurons:

During recordings, neurons were filled with fluorescent dye Alexa 568 that was added to the recording pipette solution as previously described (16). Whole-cell recordings were maintained for at least 30 min to ensure extensive cell labeling by the dye. Slices were fixed in ice-cold 4% paraformaldehyde for at least 72 h, then transferred into an anti-freeze solution (ethylene glycol and glycerol in 0.1 M phosphate buffer), and stored in the freezer. Neurons were reconstructed three-dimensionally using an Olympus Fluoview BX61 confocal microscope (Olympus America Inc, Melville, NY) with CY3 filters. Images were acquired with Fluoview software (Olympus America Inc, Melville, NY).

Proteasome Activity Assay

Chymotrypsin-like activity of the 20S proteasome was measured in WT and UCHL1 C152A knock-in mice 24 h after MCAO or sham surgery (n = 8 per group). Samples were prepared as previously described (17). Briefly, ipsilateral and contralateral penumbra were rapidly dissected out and manually homogenized and sonicated in ice-cold Tris-HCl (50 mM), pH 7.5, containing EDTA (1mM) and stored at -80°C until processing. Samples were thawed on ice, followed by centrifugation (13,000 *g*) at 4°C for 10 min. Total protein concentration was determined using a BCA protein assay. Fluorogenic substrate Suc-[Leu-Leu-Val-Tyr (LLVY)]-7-Amino-4-methylcoumarin (AMC)

cleavage was measured using a fluorescence-based assay kit (APT280, Millipore Sigma, Burlington, MA) following manufacturer's instructions.

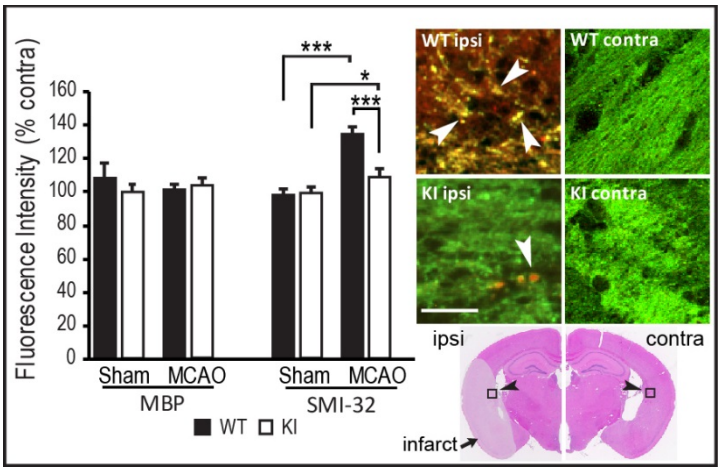

Fig. S1. White matter injury in corpus callosum 21 d post MCAO. UCHL1 C152A knock-in (KI) and wild type (WT) mice underwent 60 min. middle cerebral artery occlusion (MCAO) or sham surgery (n = 8-10 per group). Brain slices at bregma -1.9 mm were immunostained using anti-myelin basic protein (MBP, green) and anti-non-phosphorylated SMI-32 (red) antibodies. Representative images from injured animals are show in upper right panel; white arrows indicate SMI32. Fluorescence intensity was measured in ipsilateral (ipsi) and contralateral (contra) corpus callosum (400 μm x 400 μm), at the center of the infarct (black arrows, lower panel). Data are means ± SEM. * $p < 0.05$; *** $P < 0.001$, two-way ANOVA with Tukey post hoc analysis. Bar = 25 μm.

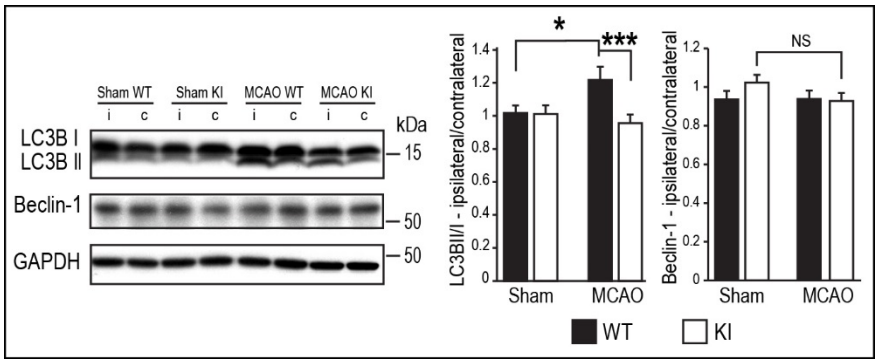

Fig. S2. Autophagy 24 h post MCAO. Male UCHL1 C152A knock-in (KI) and wild type (WT) mice underwent 60 min middle cerebral artery occlusion (MCAO) or sham surgery. Mice were sacrificed 24 h post injury and ipsilateral (i) and contralateral (c) penumbra were dissected for immunoblotting. Autophagy was examined using anti- LC3B and beclin-1 antibodies. Left: representative immunoblots; right densitometric analysis of immunoblots expressed as ipsilateral/contralateral. GAPDH was used as loading control. N = 8 - 9 per group. Data are means ± SEM. * $p < 0.05$, *** $p \leq 0.001$ with two-way ANOVA with Tukey post hoc analysis.

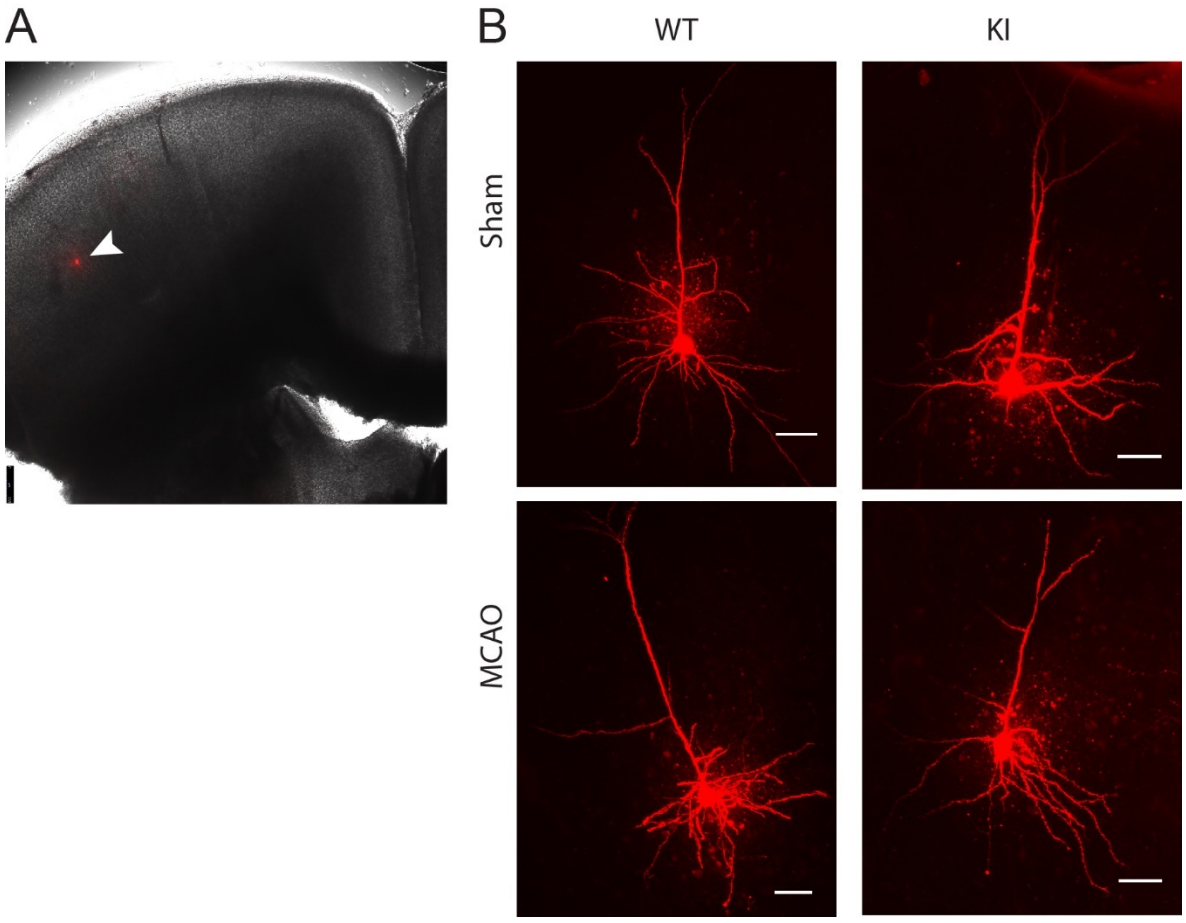

Fig. S3. A. Site of recording (white arrow). B. Representative confocal images of pyramidal neurons in 7 d post ischemia or sham wild type (WT) and UCHL1 C152A knock-in (KI) mice after injection with AlexaFluor Hydrazide 568. Bar = 20 μM.

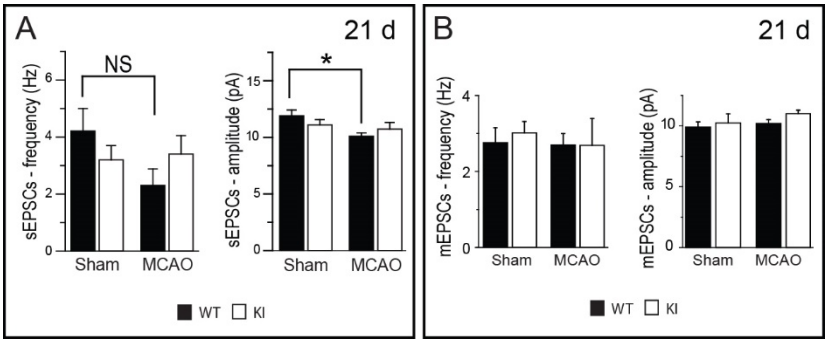

Fig. S4. Effects of MCAO on synaptic excitation in pyramidal neurons post ischemia in UCHL1 C152A knock-in (KI) and wild type (WT) mice. A. sEPSC frequency and amplitude 21 d post ischemia. N = 10-12 per group. B. mEPSC frequency and amplitude 21 d post ischemia. N = 6-12 per group. Data are means ± SEM. *P < 0.05 two-way ANOVA with Tukey post hoc testing. Black bars: WT; white bars: KI.

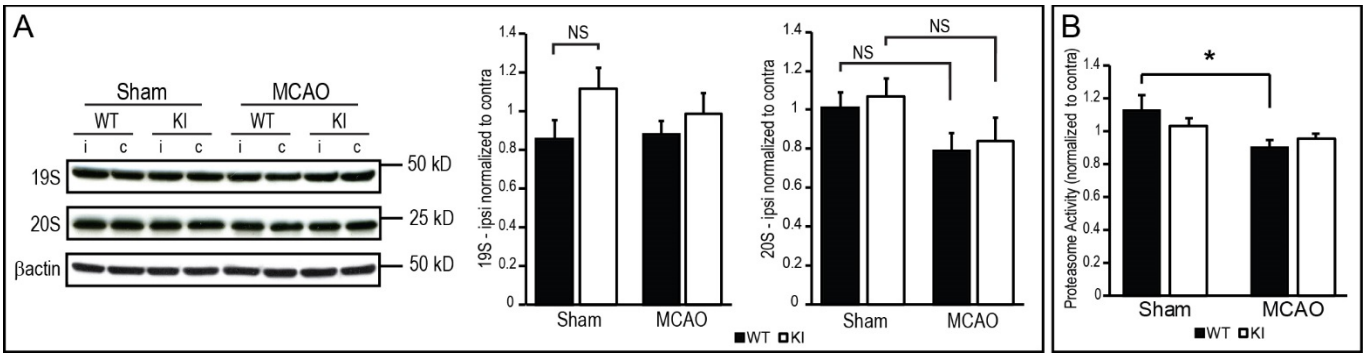

Fig. S5. Proteasome expression and activity in penumbral cortex of wild type (WT) and C152A knock-in (KI) mice 24h after sham or middle cerebral artery occlusion (MCAO) surgery. A. Immunoblots of 19S regulatory complex (n = 8-10 per group) and 20S proteasome core (n = 10 per group). β-actin was used as a loading control. B. 20S proteasome chymotrypsin-like catalytic activity as measured by cleavage of Suc-Leu-Leu-Val-Try-AMC. N = 8 per group. All: Data are means ± SEM. *P < 0.05 two-way ANOVA with Tukey post hoc testing. NS: not significant. Black bars: WT; white bars: KI.

References

1. Liu H*, et al.* (2015) Protein disulfide isomerase as a novel target for cyclopentenone prostaglandins: implications for hypoxic ischemic injury. *FEBS J* 282(10):2045-2059.
2. Cao G*, et al.* (2007) Critical role of calpain I in mitochondrial release of apoptosis-inducing factor in ischemic neuronal injury. *The Journal of neuroscience : the official journal of the Society for Neuroscience* 27(35):9278-9293.
3. Liu H*, et al.* (2015) The point mutation UCH-L1 C152A protects primary neurons against cyclopentenone prostaglandin-induced cytotoxicity: implications for post-ischemic neuronal injury. *Cell Death Dis* 6:e1966.
4. Hosie KA, King AE, Blizzard CA, Vickers JC, & Dickson TC (2012) Chronic excitotoxin-induced axon degeneration in a compartmented neuronal culture model. *ASN neuro* 4(1).
5. Fang W*, et al.* (2015) Role of the Akt/GSK-3beta/CRMP-2 pathway in axon degeneration of dopaminergic neurons resulting from MPP+ toxicity. *Brain research* 1602:9-19.
6. Jing Z*, et al.* (2014) Neuronal NAMPT is released after cerebral ischemia and protects against white matter injury. *Journal of cerebral blood flow and metabolism : official journal of the International Society of Cerebral Blood Flow and Metabolism* 34(10):1613-1621.
7. Garcia JH, Wagner S, Liu KF, & Hu XJ (1995) Neurological deficit and extent of neuronal necrosis attributable to middle cerebral artery occlusion in rats. Statistical validation. *Stroke* 26(4):627-634; discussion 635.
8. Schallert T, Fleming SM, Leasure JL, Tillerson JL, & Bland ST (2000) CNS plasticity and assessment of forelimb sensorimotor outcome in unilateral rat models of stroke, cortical ablation, parkinsonism and spinal cord injury. *Neuropharmacology* 39(5):777-787.
9. Hua Y*, et al.* (2002) Behavioral tests after intracerebral hemorrhage in the rat. *Stroke* 33(10):2478-2484.
10. Liu H*, et al.* (2017) In vivo transduction of neurons with TAT-UCH-L1 protects brain against controlled cortical impact injury. *PloS one* 12(5):e0178049.
11. Swanson RA*, et al.* (1990) A semiautomated method for measuring brain infarct volume. *Journal of cerebral blood flow and metabolism : official journal of the International Society of Cerebral Blood Flow and Metabolism* 10(2):290-293.
12. Han L*, et al.* (2015) Rosiglitazone Promotes White Matter Integrity and Long-Term Functional Recovery After Focal Cerebral Ischemia. *Stroke* 46(9):2628-2636.
13. Suenaga J*, et al.* (2015) White matter injury and microglia/macrophage polarization are strongly linked with age-related long-term deficits in neurological function after stroke. *Experimental neurology* 272:109-119.
14. Baker AJ*, et al.* (2002) Attenuation of the electrophysiological function of the corpus callosum after fluid percussion injury in the rat. *Journal of neurotrauma* 19(5):587-599.
15. Reeves TM, Phillips LL, & Povlishock JT (2005) Myelinated and unmyelinated axons of the corpus callosum differ in vulnerability and functional recovery following traumatic brain injury. *Experimental neurology* 196(1):126-137.
16. Povysheva NV*, et al.* (2006) Properties of excitatory synaptic responses in fast-spiking interneurons and pyramidal cells from monkey and rat prefrontal cortex. *Cerebral cortex* 16(4):541-552.
17. Ebrahimi-Fakhari D*, et al.* (2011) Distinct roles in vivo for the ubiquitin-proteasome system and the autophagy-lysosomal pathway in the degradation of alpha-synuclein. *The Journal of neuroscience : the official journal of the Society for Neuroscience* 31(41):14508-14520.